


Signature of a Doubly Charm Tetraquark Pole in DD^* Scattering on the LatticeM. Padmanath^{1,2,*} and S. Prelovsek^{3,4,†}¹Helmholtz Institut Mainz, Staudingerweg 18, 55128 Mainz, Germany²GSI Helmholtzzentrum für Schwerionenforschung GmbH, Planckstr. 1, 64291 Darmstadt, Germany³Faculty of Mathematics and Physics, University of Ljubljana, 1000 Ljubljana, Slovenia⁴Jozef Stefan Institute, 1000 Ljubljana, Slovenia (Received 2 March 2022; revised 19 April 2022; accepted 24 June 2022; published 12 July 2022)

The doubly charm tetraquark with flavor $cc\bar{u}\bar{d}$ and isospin $I = 0$ is investigated by calculating the DD^* scattering amplitude with lattice QCD. The simulation is done on CLS ensembles with dynamical $u/d, s$ quarks and $m_\pi \simeq 280$ MeV for two charm quark masses, one slightly larger and one slightly lower than the physical value. The scattering amplitudes for partial waves $l = 0, 1$ are extracted near threshold via the Lüscher method by considering systems with total momenta $PL/(2\pi) = 0, 1, \sqrt{2}, 2$ on two spatial volumes. A virtual bound state pole in the DD^* scattering amplitude with $l = 0$ is found $9.9^{+3.6}_{-7.1}$ MeV below the DD^* threshold for the charm quark mass closer to the physical value. This pole is likely related to the doubly charm tetraquark discovered by LHCb less than 1 MeV below the D^0D^{*+} threshold. Future lattice simulations closer to the continuum limit and physical quark masses would be valuable to establish this connection systematically.

DOI: [10.1103/PhysRevLett.129.032002](https://doi.org/10.1103/PhysRevLett.129.032002)

Introduction.—The LHCb Collaboration recently discovered a doubly charmed tetraquark T_{cc} with flavor $cc\bar{u}\bar{d}$ just 0.36(4) MeV below D^0D^{*+} threshold [1–3]. Its flavor is based on the decay channel $D^0D^0\pi^+$, and it has isospin $I = 0$ since no state was found in the decay $D^0D^+\pi^+$. The total spin and parity J^P have not been determined from experiment. This is the longest-lived hadron discovered with explicitly exotic quark content. It has striking similarities with the well-known $X(3872)$ [4] that lies very close to $D^0\bar{D}^{*0}$ threshold. Here we aim at the theoretical investigation of near-threshold exotics from first principles.

Several phenomenological models predicted a doubly charm tetraquark $cc\bar{u}\bar{d}$ with $I = 0$ and $J^P = 1^+$ within an energy range ± 100 MeV around the DD^* threshold, e.g., Refs. [5–13]. Many of these models have the possibility to identify a bound state but not a resonance. One of the more sophisticated quark model calculations predicted the bound state 1.6 ± 1.0 MeV below DD^* threshold and concluded that the molecular Fock component dominates over the diquark-antidiquark component [12]. Within a molecular picture, a light vector meson exchange is argued to induce attraction [14,15], whereas one-pion exchange induces slight repulsion [16]. The binding energy of a bound state in the $QQ\bar{u}\bar{d}$ system is found to decrease

with decreasing heavy quark mass m_Q and with increasing light quark mass $m_{u,d}$ [10,12,17–25]. Thus, the doubly bottom tetraquarks $bb\bar{u}\bar{d}$ and $bb\bar{u}\bar{s}$ with $J^P = 1^+$ are deeply bound according to a variety of theoretical approaches [10,12,17–19,21,22,24], whereas $cc\bar{u}\bar{d}$ is expected on the verge of binding and requires a careful theoretical study within QCD.

In order to theoretically confirm the existence of a doubly charmed tetraquark from first principles, one has to establish a pole in the corresponding scattering amplitude $t(E_{\text{cm}})$ that depends on the center-of-momentum (cm) energy. This is particularly important in finite-volume formulations, such as lattice QCD, since this state does not lie well below the threshold but is expected near threshold. Lattice QCD represents the only nonperturbative first-principles approach with quantifiable systematic and statistical uncertainties to study QCD in the hadronic regime. It enables the determination of the scattering amplitudes from deviations of finite-volume energies from the noninteracting scenario [26]. However, the scattering amplitude in this channel has not been determined using lattice simulations yet. The lattice study in Ref. [17] extracted the finite-volume energy of the ground state using meson-meson and diquark-antidiquark interpolators for a wide range of $m_\pi \geq 260$ MeV and three lattice spacings. The continuum and chiral extrapolations led to an energy level -23 ± 11 MeV relative to the DD^* threshold. This indicates the presence of interactions between D and D^* but does not prove the existence of a pole. The finite-volume energies have been extracted in Ref. [27], and the ground state energy was found to be consistent with the DD^* threshold.

Published by the American Physical Society under the terms of the [Creative Commons Attribution 4.0 International license](https://creativecommons.org/licenses/by/4.0/). Further distribution of this work must maintain attribution to the author(s) and the published article's title, journal citation, and DOI. Funded by SCOAP³.

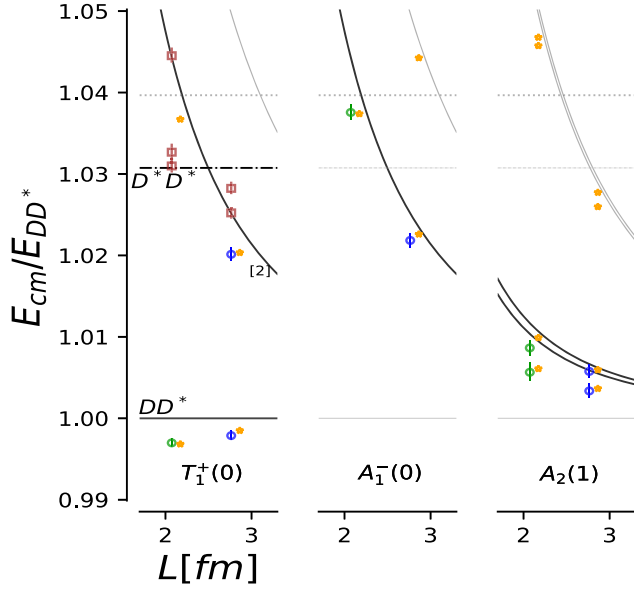


FIG. 1. Center-of-momentum energy $E_{\text{cm}} = (E^2 - \vec{P}^2)^{1/2}$ of the $cc\bar{u}\bar{d}$ system normalized by $E_{DD^*} \equiv m_D + m_{D^*}$, for the heavier charm quark mass in various finite-volume irreps. The lattice energy levels are shown by large circles and squares: The scattering analysis employs the blue and green circles. The noninteracting DD^* energies (1) are shown by lines: The operators related to black lines are employed, while those related to gray lines are omitted. Label [2] in $T_1^+(0)$ refers to the multiplicity of noninteracting level $D(1)D^*(1)$. The orange stars represent the analytically reconstructed energy levels based on the fitted scattering amplitudes and are slightly horizontally shifted for clarity.

This Letter investigates if a state with flavor $cc\bar{u}\bar{d}$, $I = 0$, and $J^P = 1^+$ exists in the vicinity of DD^* threshold. For this purpose, the DD^* scattering amplitude $t(E_{\text{cm}})$ near threshold is extracted within lattice QCD for the first time. It is determined from finite-volume energies via the Lüscher method [26]. The D^* does not decay strongly to $D\pi$ at the simulated $m_\pi \simeq 280$ MeV, and the analyzed energy region is below the $DD\pi$ and D^*D^* thresholds; therefore, we consider one-channel DD^* scattering. We demonstrate that the scattering amplitude indeed has a pole at E_{cm}^p slightly below threshold.

TABLE I. Total momenta \vec{P} , spatial lattice symmetry group (LG), irreducible representations (Λ^P), and interpolators considered for the system $cc\bar{u}\bar{d}$, together with total spin-parity J^P and partial wave l of DD^* scattering that contributes to each irrep (only $J, l \leq 2$ are listed). The interpolators are denoted by [2] when two linearly independent combinations of momenta and polarizations are employed, e.g., $O_{l=0,2}$ for $D(1)D^*(1)$ in T_1^+ [32].

ID	\vec{P}	LG	Λ^P	J^P	l	Interpolators: $M_1(\vec{p}_1^2)M_2(\vec{p}_2^2)$
1	(0,0,0)	O_h	T_1^+	1^+	0,2	$D(0)D^*(0), D(1)D^*(1)[2], D^*(0)D^*(0)$
2	(0,0,0)	O_h	A_1^-	0^-	1	$D(1)D^*(1)$
3	(0, 0, 1)($2\pi/L$)	Dic_4	A_2	$0^-, 1^+, 2^-$	0,1,2	$D(0)D^*(1), D(1)D^*(0)$
4	(1, 1, 0)($2\pi/L$)	Dic_2	A_2	$0^-, 1^+, 2^-, 2^+$	0,1,2	$D(0)D^*(2), D(1)D^*(1)[2], D(2)D^*(0)$
5	(0, 0, 2)($2\pi/L$)	Dic_4	A_2	$0^-, 1^+, 2^-$	0,1,2	$D(1)D^*(1)$

First we present the calculation of the energy levels. Then we discuss the extraction of the scattering amplitude and the poles in it.

Ensembles and single-hadron masses.—We utilize two ensembles with $u/d, s$ dynamical quarks provided by the Coordinated Lattice Simulations consortium [28,29]. The lattice spacing is $a = 0.08636(98)(40)$ fm, and m_u and m_d are degenerate and heavier than in nature, corresponding to $m_\pi = 280(3)$ MeV. There are 255 configurations on spatial volume $N_L^3 = 24^3$ and 492 configurations on 32^3 [30]. The scattering amplitude is extracted for two values of the charm quark mass, one slightly heavier than physical and one slightly lighter [31]. The masses of the relevant hadrons D and D^* are presented in Table II. The heavier charm quark mass is closer to the physical value and provides our main result.

Interpolators and finite-volume energies.—In the non-interacting limit, the DD^* system has discrete energies on a periodic lattice of size $L = N_L a$,

$$E^{\text{ni}} = E_{D(\vec{p}_1)} + E_{D^*(\vec{p}_2)}, \quad \vec{p}_i = \vec{n}_i \frac{2\pi}{L}, \quad \vec{n}_i \in N_L^3 \quad (1)$$

with $E_{H(\vec{p}_i)}^{\text{con}} = (m_H^2 + \vec{p}_i^2)^{1/2}$ in the continuum limit. The noninteracting energies are shown by lines in Fig. 1.

The finite-volume energies in the interacting theory are determined from the correlation matrices $C_{ij}(t) = \langle O_i(t_{\text{src}} + t) O_j^\dagger(t_{\text{src}}) \rangle$, where O_i refers to operators that annihilate states with the desired quantum numbers. The $cc\bar{u}\bar{d}$ system is investigated in inertial frames with total momenta $|\vec{P}|L/(2\pi) = 0, 1, \sqrt{2}, 2$ and finite-volume irreducible representations (irreps) in Table I. These constrain DD^* scattering in various partial waves l , of which $l = 0$ is expected to dominate near threshold. We utilize only meson-meson interpolators, where each meson is projected to a definite momentum,

$$\begin{aligned} O^{DD^*} &= \sum_{k,j} A_{kj} D(\vec{p}_{1k}) D_j^*(\vec{p}_{2k}), \quad \vec{p}_{1k} + \vec{p}_{2k} = \vec{P} \\ &= \sum_{k,j} A_{kj} [(\bar{u}\Gamma_1 c)_{\vec{p}_{1k}} (\bar{d}\Gamma_2 j c)_{\vec{p}_{2k}} - (\bar{d}\Gamma_1 c)_{\vec{p}_{1k}} (\bar{u}\Gamma_2 j c)_{\vec{p}_{2k}}] \end{aligned} \quad (2)$$

TABLE II. Lattice results for the binding energy $\delta m_{T_{cc}}$ and the effective range parameters in Eq. (3) at heavier ($m_c^{(h)}$) and lighter ($m_c^{(l)}$) charm quark masses, compared to experiment. Note that $m_c^{(h)}$ is closer to the physical value according to the spin averaged charmonium mass $M_{av} \equiv (1/4)(m_{\eta_c} + 3m_{J/\psi})$. The real part of experimental $a_0^{(1)}$ is provided. The binding energy $\delta m_{T_{cc}} \equiv \text{Re}(E_{cm}^p) - m_{D^0} - m_{D^{*+}}$ is obtained from the energy E_{cm}^p , where the scattering amplitude has a pole. Lattice results are shown with 1σ statistical errors at given quark masses and lattice spacing; the T_{cc} is found to be a virtual bound state with $\delta m_{T_{cc}} < 0$ also within 2σ and 3σ error ranges.

	m_D (MeV)	m_{D^*} (MeV)	M_{av} (MeV)	$a_{l=0}^{(J=1)}$ (fm)	$r_{l=0}^{(J=1)}$ (fm)	$\delta m_{T_{cc}}$ (MeV)	T_{cc}
Lattice ($m_\pi \simeq 280$ MeV, $m_c^{(h)}$)	1927(1)	2049(2)	3103(3)	1.04(29)	0.96 $^{(+0.18)}_{(-0.20)}$	-9.9 $^{+3.6}_{-7.2}$	Virtual bound st.
Lattice ($m_\pi \simeq 280$ MeV, $m_c^{(l)}$)	1762(1)	1898(2)	2820(3)	0.86(0.22)	0.92 $^{(+0.17)}_{(-0.19)}$	-15.0 $^{(+4.6)}_{(-9.3)}$	Virtual bound st.
Experiment [2,41]	1864.85(5)	2010.26(5)	3068.6(1)	-7.15(51)	[-11.9(16.9), 0]	-0.36(4)	Bound st.

with two choices $(\Gamma_1, \Gamma_{2j}) = (\gamma_5, \gamma_j), (\gamma_5\gamma_t, \gamma_j\gamma_t)$ throughout. Operators are shown in Sec. I of Ref. [32]. All quark fields are smeared according to the ‘‘distillation’’ method [31,40] with 60(90) Laplacian eigenvectors for $N_L = 24(32)$.

The diquark-antidiquark interpolators $[cc][\bar{d}\bar{u}]$ are not considered in this Letter. This is justified as it was observed in an earlier lattice calculation that such operators have negligible effects on the low-lying energies [27]. Indications from phenomenological studies on the dominance of molecular DD^* Fock components [12] also suggest that DD^* interpolators are sufficient to compute the energies faithfully. Furthermore, the application of two operators $D_{\gamma_5}D_{\gamma_j}^*$ and $D_{\gamma_5\gamma_t}D_{\gamma_j\gamma_t}^*$ for each momentum combination is expected to provide enough variety to extract the energy levels reliably.

The energies E_n^{lat} are extracted from single-exponential fits to the eigenvalue correlators $\lambda^{(n)}(t) \propto e^{-E_n^{\text{lat}}t}$ of the generalized eigenvalue problem $C(t)v^{(n)}(t) = \lambda^{(n)}(t) \times C(t_0)v^{(n)}(t)$ with $t_0 = 4$ [42]. In order to mitigate small deviations of single-hadron energies $E_{H(\vec{p})}^{\text{lat}}$ from $E_{H(\vec{p})}^{\text{con}}$ due to discretization effects, we take $E_n = E_n^{\text{lat}} + E_{D(\vec{p}_1)}^{\text{con}} + E_{D^*(\vec{p}_2)}^{\text{con}} - E_{D(\vec{p}_1)}^{\text{lat}} - E_{D^*(\vec{p}_2)}^{\text{lat}}$ as the final energies for the scattering analysis, as argued and utilized on the same ensembles in Refs. [31,33].

The resulting finite-volume energies in the first three irreps are presented in Fig. 1 for the heavier charm quark mass. The figure displays the energies $E_{cm} = (E^2 - \vec{P}^2)^{1/2}$ in the center-of-momentum frame in units of energy of the DD^* threshold. The large circles and squares refer to the energy levels extracted from the lattice simulation. The energy levels have nonzero energy shifts with respect to the noninteracting DD^* energies, indicating nontrivial interactions. These energy shifts render information on the DD^* scattering amplitudes. We find similar observations at the lighter charm quark mass [32].

Scattering analysis.—The scattering amplitude t in $S = e^{2i\delta} = 1 + i(4p/E_{cm})t$ depends on energy, the partial wave l , and $J = |s - l|, \dots, |s + l|$, where $s = 1$ for the DD^* system. We approximate their energy dependence near threshold with two terms of the effective range expansion in p^2 ([43])

$$t_l^{(J)} = \frac{E_{cm}}{2} \frac{1}{p \cot \delta_l^{(J)} - ip}, \quad p^{2l+1} \cot \delta_l^{(J)} = \frac{1}{a_l^{(J)}} + \frac{r_l^{(J)}}{2} p^2, \quad (3)$$

where $p = |\vec{p}|$ is the spatial momentum of D and D^* in the center-of-momentum frame. Each finite-volume energy level E_{cm} is related to the $t_l^{(J)}(E_{cm})$ via Lüscher’s relation [26] and its generalizations, e.g., Ref. [34]. In order to constrain the energy dependence of t , the parameters of the effective range expansion are optimized such that Lüscher’s relation is simultaneously satisfied for all the energy levels considered. For the $l = 0$ partial wave, which dominates near threshold, we find

$$p \cot \delta_{l=0}^{(J=1)} = \frac{1}{a_0^{(1)}} + \frac{1}{2} r_0^{(1)} p^2, \quad m_c^{(h)} : a_0^{(1)} = 1.04(29) \text{ fm}, \quad r_0^{(1)} = 0.96^{(+0.18)}_{(-0.20)} \text{ fm}. \quad (4)$$

This fit is shown by the red line in Fig. 2.

This result is robust to various fits we have performed, as further detailed in Ref. [32]. The $J^P = 1^+$ is allowed for the DD^* system with spin one in partial waves $l = 0$ and $l = 2$, which could lead to a partial wave mixing. We find that $t_2^{(1)}$ is consistent with zero since the energy levels with dominant overlaps to $O_{l=2}$ [32] have energies consistent with the noninteracting energy (1). Hence, we assume $t_{l \geq 2}^{(J)} = 0$ and negligible mixing of $l = 2$ with $l = 0$ in $J = 1$ [32]. The energies in blue and green from Fig. 1 are utilized to constrain the energy dependence of $t_0^{(1)}$ in Eq. (4) and $t_1^{(0)}$. We employ a combination of procedures outlined in Refs. [35,36] in making our fits [32]. The fit has $\chi^2/\text{dof} = 3.7/5$ and renders the parameters in Eq. (4) for $l = 0$ scattering and $[a_1^{(0)} = 0.076^{(+0.008)}_{(-0.009)} \text{ fm}^3, r_1^{(0)} = 6.9(2.1) \text{ fm}^{-1}]$ for $l = 1$ scattering. The fit results for $t_1^{(0)}$ render poles significantly below threshold, at energies that are unconstrained by the energy levels, and therefore we do not ascribe them any physical significance. The analytically reconstructed energies based on these t_l^J are indicated by

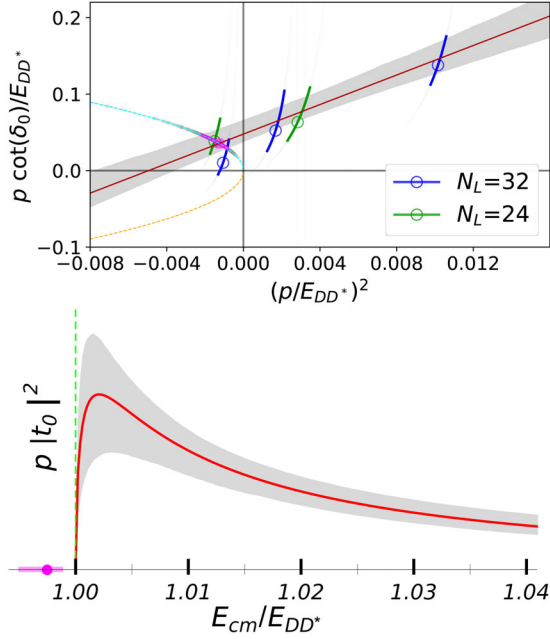


FIG. 2. Top: $p \cot \delta_{l=0}^{(J=1)}$ for DD^* scattering at the heavier charm quark mass (red line) and $ip = +|p|$ (cyan line) versus p^2 , all normalized to $E_{DD^*} \equiv m_D + m_{D^*}$. The virtual bound state occurs at the momenta indicated by the magenta octagon, where two curves intersect. Bottom: corresponding DD^* scattering rate $N \propto p |t_0|^2$ above threshold along with the pole position.

orange stars in Fig. 1 and agree well with the observed energies.

The pole in the DD^ scattering amplitude and T_{cc} .*— Before focusing on T_{cc} , let us briefly review the relation between hadrons and poles. The existence a hadron state and its mass is inferred from the pole in the scattering amplitude $t(E_{cm})$. The bound state and the virtual bound state have a pole at a real energy below threshold, and therefore $p^2 < 0$. A bound state has a pole at $p = i|p_B|$ and is an asymptotic state, e.g., deuteron. A virtual bound state has a pole at $p = -i|p_B|$ and is less familiar; it appears, for example, in an 1S_0 nucleon-nucleon channel [32,37,38]. Finally, the most common poles with E_{cm} away from the real axis correspond to decaying resonances, e.g., ρ meson.

We find a virtual bound state pole in the DD^* scattering amplitude $t_{l=0}^{(J=1)}$ at energy $E_{cm}^p = (m_D^2 - |p_B|^2)^{1/2} + (m_{D^*}^2 - |p_B|^2)^{1/2}$. It corresponds to the binding momentum indicated by the magenta octagon in Fig. 2. We therefore find evidence for the doubly charmed tetraquark as a virtual bound state with binding energy

$$m_c^{(h)}: \delta m_{T_{cc}} = E_{cm}^p - m_D - m_{D^*} = -9.9_{-7.1}^{+3.6} \text{ MeV}. \quad (5)$$

It is situated slightly below DD^* threshold, close to the mass of the doubly charmed tetraquark T_{cc} discovered by LHCb [1,2]. The state found on the lattice is strongly stable, and the pole appears at real energy since $D^* \rightarrow D\pi$ is not

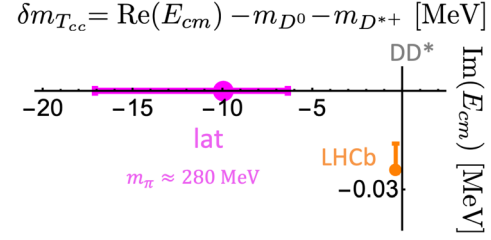


FIG. 3. Pole in the scattering amplitude related to T_{cc} in the complex energy plane: our lattice result at the heavier charm quark mass (magenta) and the LHCb result (orange).

kinematically allowed for $m_\pi \simeq 280$ MeV. The T_{cc} discovered by LHCb decays to $D^0 D^0 \pi^+$, and the pole is slightly imaginary, as shown in Fig. 3. The T_{cc} found in experiment would be a bound state in the limit of stable D^{*+} since the measured $a_0^{(1)}$ is negative [2].

The quark mass dependence of T_{cc} and the notion of a virtual bound state can be most easily illustrated for s -wave scattering in a purely attractive potential $V(r)$ within quantum mechanics. Explicit toy-model examples are given in Refs. [32]. The bound state occurs at $p = i|p_B|$; its wave function falls as $e^{ipr} = e^{-|p_B|r}$ outside the potential and is an asymptotic state. As the potential depth is weakened, the bound state energy approaches threshold. As the potential is weakened even further so that it is not attractive enough to form a bound state, the s -wave bound state typically becomes a virtual bound state. It occurs at $p = -i|p_B|$, and its wave function $e^{ipr} = e^{|p_B|r}$ outside V is not normalizable; therefore, it is not an asymptotic state. Even so, it gives rise to an abrupt enhancement in the scattering cross section above the threshold when the pole is close below threshold. This enhancement is shown in Fig. 2 for DD^* scattering and appears due to the virtual bound state T_{cc} in our study.

We expect that the virtual bound state pole found in our lattice simulation at unphysical u/d masses is related to the T_{cc} discovered by LHCb, as detailed in Sec. IV of Ref. [32]. The would-be LHCb bound state is expected to become a virtual bound state with increasing $m_{u/d}$. This is sketched in Fig. 4 for a tetraquark with a significant molecular DD^* component attracted by the Yukawa-like potential

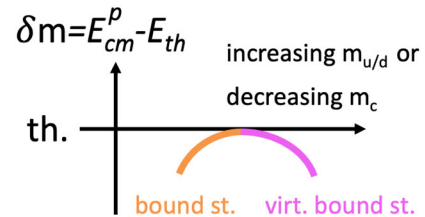


FIG. 4. Sketch of the binding energy for the (virtual) bound state dominated by the molecular component. It is based on a purely attractive potential $V(r)$ and partial wave $l = 0$ within quantum mechanics.

$V(r) \propto e^{-Mr}/r$, where the mass of the exchanged light hadron M increases with increasing $m_{u/d}$.

A near-threshold virtual bound state pole is also observed for the lighter charm quark mass with a slightly larger $|\delta m_{T_{cc}}|$, as listed in Table II. This observation is consistent with the dependence of pole position on m_c sketched in Fig. 4. This arises within quantum mechanics via the reduced DD^* mass for a purely attractive potential $V(r)$ that is assumed to be flavor blind [44].

Conclusions.—We have performed a simulation of DD^* scattering in lattice QCD at $m_\pi \simeq 280$ MeV. Unlike other existing lattice investigations in this regard, we extracted the near-threshold scattering amplitudes in the flavor channel $cc\bar{u}\bar{d}$ with isospin $I = 0$. Scattering amplitudes for partial waves $l = 0, 1$ are determined via Lüscher's method, and a virtual bound state pole is found for the partial wave $l = 0$. The doubly charm tetraquark with $J^P = 1^+$ features as a virtual bound state $9.9^{+3.6}_{-7.1}$ MeV below threshold in our simulation, that has charm quark mass slightly larger than physical. We also observe that the size of the binding energy for this virtual bound state increases with decreasing charm quark mass.

Outlook.—Future lattice studies are desired to reaffirm our findings and inferences. The current knowledge could be improved by adding diquark-antidiquark interpolators, exploring the dependence on quark masses, and investigating discretization effects based on improved actions and at smaller lattice spacings. The simulations at smaller $m_{u/d}$ are required to establish whether the pole will approach the DD^* threshold. The simulations at physical $m_{u/d}$ will be challenging due to the strong decays $D^* \rightarrow D\pi$ and $T_{cc} \rightarrow DD\pi$, while the formalism is already available in Ref. [46].

We would particularly like to thank Sara Collins and the members of the RQCD Collaboration for discussions and support related to the computer resources used in this project. We are grateful to J. J. Dudek, J. R. Green, F.-K. Guo, A. D. Hanlon, B. Hörz, M. Karliner, L. Leskovec, M. Mai, N. Mathur, D. Mohler, E. Oset, S. Paul, M. Rosina, M. Sadl, S. Sharpe, and B.-S. Zou for valuable discussions. We thank our colleagues at CLS for the joint effort in the generation of the gauge field ensembles which form a basis for the computation. The correlators were computed on the Regensburg Athene2 cluster. We thank the authors of Ref. [35] for making the *TwoHadronsInBox* package public and C. B. Lang for contributions to the computing codes we used. S.P. acknowledges support by Slovenian Research Agency ARRS (Research Core Funding No. P1-0035).

*pmadanag@uni-mainz.de,

pappan@gmail.com

†sasa.prelovsek@ijs.si

[1] R. Aaij *et al.* (LHCb Collaboration), Nat. Phys. (2022). 10.1038/s41567-022-01614-y.

- [2] R. Aaij *et al.* (LHCb Collaboration), Nat. Commun. **13**, 3351 (2022).
- [3] The mass obtained from the pole position in Ref. [2] is quoted.
- [4] S. K. Choi *et al.* (Belle Collaboration), Phys. Rev. Lett. **91**, 262001 (2003).
- [5] J. P. Ader, J. M. Richard, and P. Taxil, Phys. Rev. D **25**, 2370 (1982).
- [6] L. Heller and J. A. Tjon, Phys. Rev. D **35**, 969 (1987).
- [7] J. Carlson, L. Heller, and J. A. Tjon, Phys. Rev. D **37**, 744 (1988).
- [8] F. S. Navarra, M. Nielsen, and S. H. Lee, Phys. Lett. B **649**, 166 (2007).
- [9] D. Ebert, R. N. Faustov, V. O. Galkin, and W. Lucha, Phys. Rev. D **76**, 114015 (2007).
- [10] M. Karliner and J. L. Rosner, Phys. Rev. Lett. **119**, 202001 (2017).
- [11] E. J. Eichten and C. Quigg, Phys. Rev. Lett. **119**, 202002 (2017).
- [12] D. Janc and M. Rosina, Few-Body Syst. **35**, 175 (2004).
- [13] T. F. Carames, A. Valcarce, and J. Vijande, Phys. Lett. B **699**, 291 (2011).
- [14] A. Feijoo, W. H. Liang, and E. Oset, Phys. Rev. D **104**, 114015 (2021).
- [15] X.-K. Dong, F.-K. Guo, and B.-S. Zou, Commun. Theor. Phys. **73**, 125201 (2021).
- [16] M.-L. Du, V. Baru, X.-K. Dong, A. Filin, F.-K. Guo, C. Hanhart, A. Nefediev, J. Nieves, and Q. Wang, Phys. Rev. D **105**, 014024 (2022).
- [17] P. Junnarkar, N. Mathur, and M. Padmanath, Phys. Rev. D **99**, 034507 (2019).
- [18] M. Pflaumer, L. Leskovec, S. Meinel, and M. Wagner, Proc. Sci., LATTICE2021 (2022) 392.
- [19] A. Francis, R. J. Hudspith, R. Lewis, and K. Maltman, Phys. Rev. Lett. **118**, 142001 (2017).
- [20] A. Francis, R. J. Hudspith, R. Lewis, and K. Maltman, Phys. Rev. D **99**, 054505 (2019).
- [21] L. Leskovec, S. Meinel, M. Pflaumer, and M. Wagner, Phys. Rev. D **100**, 014503 (2019).
- [22] B. Colquhoun, A. Francis, R. J. Hudspith, R. Lewis, and K. Maltman, Proc. Sci., LATTICE2021 (2022) 144..
- [23] R. J. Hudspith, B. Colquhoun, A. Francis, R. Lewis, and K. Maltman, Phys. Rev. D **102**, 114506 (2020).
- [24] P. Bicudo, K. Cichy, A. Peters, B. Wagenbach, and M. Wagner, Phys. Rev. D **92**, 014507 (2015).
- [25] A. Francis, P. de Forcrand, R. Lewis, and K. Maltman, J. High Energy Phys. **05** (2022) 062.
- [26] M. Luscher, Nucl. Phys. **B354**, 531 (1991).
- [27] G. K. C. Cheung, C. E. Thomas, J. J. Dudek, and R. G. Edwards (Hadron Spectrum Collaboration), J. High Energy Phys. **11** (2017) 033.
- [28] M. Bruno *et al.*, J. High Energy Phys. **02** (2015) 043.
- [29] G. S. Bali, E. E. Scholz, J. Simeth, and W. Söldner (RQCD Collaboration), Phys. Rev. D **94**, 074501 (2016).
- [30] M. Bruno, T. Korzec, and S. Schaefer, Phys. Rev. D **95**, 074504 (2017).
- [31] S. Piemonte, S. Collins, D. Mohler, M. Padmanath, and S. Prelovsek, Phys. Rev. D **100**, 074505 (2019).
- [32] See Supplemental Material at <http://link.aps.org/supplemental/10.1103/PhysRevLett.129.032002> for the

details of the operators utilized, the fitting procedure, the results from amplitude fits, and a discussion on the heavy quark mass dependence of the near-threshold state. This includes Refs. [9,11,16–19,21,23,24,29,33–39], Supplemental Material video file. Demonstration of trajectory of the pole singularity in an attractive Gaussian potential $V = -V_0 e^{-r^2/R^2}$.

- [33] S. Prelovsek, S. Collins, D. Mohler, M. Padmanath, and S. Piemonte, *J. High Energy Phys.* **06** (2021) 035.
- [34] R. A. Briceno, *Phys. Rev. D* **89**, 074507 (2014).
- [35] C. Morningstar, J. Bulava, B. jit Singha, R. Brett, J. Fallica, A. Hanlon, and B. Hörz, *Nucl. Phys.* **B924**, 477 (2017).
- [36] A. J. Woss, D. J. Wilson, and J. J. Dudek (Hadron Spectrum Collaboration), *Phys. Rev. D* **101**, 114505 (2020).
- [37] I. Matuschek, V. Baru, F.-K. Guo, and C. Hanhart, *Eur. Phys. J. A* **57**, 101 (2021).
- [38] P. Reinert, H. Krebs, and E. Epelbaum, *Eur. Phys. J. A* **54**, 86 (2018).
- [39] S. Prelovsek, U. Skerbis, and C. B. Lang, *J. High Energy Phys.* **01** (2017) 129.
- [40] M. Peardon, J. Bulava, J. Foley, C. Morningstar, J. Dudek, R. G. Edwards, B. Joó, H.-W. Lin, D. G. Richards, and K. J. Juge (Hadron Spectrum Collaboration), *Phys. Rev. D* **80**, 054506 (2009).
- [41] P. Zyla *et al.* (Particle Data Group), *Prog. Theor. Exp. Phys.* **2020**, 083C01 (2020).
- [42] C. Michael, *Nucl. Phys.* **B259**, 58 (1985).
- [43] This relation omits mixing of partial waves for reasons discussed later, while the more general relation is provided in Ref. [32].
- [44] Otherwise, the lattice results for the binding energy at various heavy quark masses can be used to examine how good the heavy flavor symmetry is, in line with Ref. [45].
- [45] V. Baru, E. Epelbaum, J. Gegelia, C. Hanhart, U.-G. Meißner, and A. V. Nefediev, *Eur. Phys. J. C* **79**, 46 (2019).
- [46] T. D. Blanton and S. R. Sharpe, *Phys. Rev. D* **104**, 034509 (2021).